Liquid crystal lens array for 3D microscopy and endoscope application

Yi-Pai Huang[1], Po-Yuan Hsieh[1], Amir Hassanfiroozi[1], Chao-Yu Chu[1], Yun Hsuan[1], Manuel Martinez[2], Bahram Javidi[3]
[1]Department of Photonics & Institute of Electro-Optical Engineering & Display Institute, National Chiao Tung University, Hsinchu, TAIWAN
[2]Department of Physics, University of Valencia, Valencia, SPAIN
[3]Electrical and Computer Engineering Department, University of Connecticut, Storrs, CT, USA

ABSTRACT

In this paper, we demonstrate two liquid crystal (LC) lens array devices for 3D microscope and 3D endoscope applications respectively. Compared with the previous 3D biomedical system, the proposed LC lens arrays are not only switchable between 2D and 3D modes, but also are able to adjust focus in both modes. The multi-function liquid crystal lens (MFLC-lens) array with dual layer electrode has diameter 1.42 mm, which is much smaller than the conventional 3D endoscope with double fixed lenses. The hexagonal liquid crystal micro-lens array (HLC-MLA) instead of fixed micro-lens array in 3D light field microscope can extend the effective depth of field from 60 um to 780 um. To achieve the LC lens arrays, a high-resistance layer needs to be coated on the electrodes to generate an ideal gradient electric-field distribution, which can induce a lens-like form of LC molecules. The parameters and characteristics of high-resistance layer are investigated and discussed with an aim to optimize the performance of liquid crystal lens arrays.

Keywords: Liquid Crystal Lens Array, Light Field Microscopy, Extend Depth of Focus, 3D Endoscope

1. INTRODUCTION

1.1 Liquid crystal lens

Liquid crystal (LC) lenses are active optical elements with electrically tunable focal lengths without any mechanical movements. Because of the large optical anisotropy of this material, the LC director's orientation can be easily controlled by applying low voltage to a nematic liquid crystal. When an incident plane wave passes through a lens-like phase difference of LC directors, the wave will be converged or diverged depending on the type of voltage applied to the electrodes. The early reports on LC lenses [1-3] used a ratio of the diameter to the cell thickness of about 2~3 for an LC lens optimized to work like a lens. To further improve the optical performance of LC lens, a high-dielectric layer [4-5] was used to smooth the phase profile across the lens without attenuating much electrical potential. However, high-dielectric layer increases the operating voltage to higher than 30 volts. Therefore, high-resistive layer [6-7] was applied to generate linearly varying electrical potential from the center to the edge. The high-resistive layer for LC lens successfully demonstrated low operating voltage, fast response time, and high optical performance.

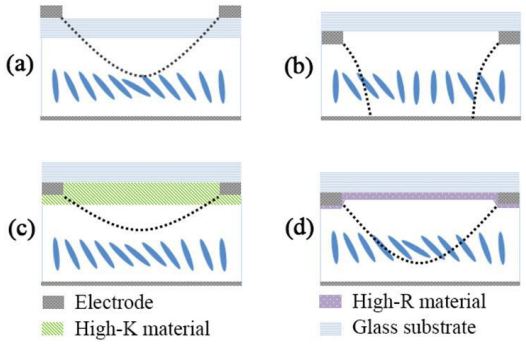

Figure 1. The cross-section of different LC lens, (a) external electrode LC lens, (b) internal electrode LC lens, (c) LC lens using a high-K layer, (d) LC lens using a high-R layer. The dashed line shows the potential.

Three-Dimensional Imaging, Visualization, and Display 2016, edited by Bahram Javidi, Jung-Young Son, Proc. of SPIE
Vol. 9867, 98670W · © 2016 SPIE · CCC code: 0277-786X/16/$18 · doi: 10.1117/12.2229452

The orientation of LC directors is determined by potential differences across the two conductive layers at the top and bottom of the liquid crystal. This can change LC lens properties. To make a lens-like effect in a liquid crystal cell a hole-patterned electrode on the glass is designed as shown in Figure 1(a). However, high driving voltages are required to make a gradient potential from the edge of the LC lens to the center of the LC lens, due to the shielding of the voltage in the glass substrate. If the electrode's position is upside-down as in Figure 1(b), the required driving voltage is lower, but there is no lens-like distribution of the refractive index. The applied voltages can be lowered using a high dielectric (high-k) layer coated on the hole-patterned electrode to smooth the phase profile across the lens, though a lower applied voltage is still desired. Because of the thickness of this layer (~few um), high-K layer shields a portion of the applied voltage as in Figure 1(c). This problem can be solved by using a thin film layer with high-resistivity (high-R) as in Figure 1(d), which also provides more options to fabricate an LC lens according to aperture size. By adjusting to a proper frequency, the aperture becomes larger the driving frequency becomes lower. When the aperture is small, a higher driving frequency is needed. Thus, making LC lenses with various sizes will be possible with a very low driving voltage.

2. 3D ENDOSCOPE

Conventional endoscopic systems consisting of several solid lenses suffer from a fixed lens. For practical applications using conventional endoscopes, the doctor may have to move the endoscope back and forth during the examination in order to see a clear image, which may make the patient uncomfortable. 3D vision offers the advantage of improved depth perception and accuracy in the performance of endoscopic surgery, particularly for complex surgical tasks such as suturing [8].

As shown in Figure 2, the proposed multi-functional LC lens (MFLC-lens) is able to switch to and from 2D and 3D modes, and can further change the focus in both modes. The system is investigated by using dual-layer electrodes and a high resistive transparent film. The high resistance film is used to minimize the electric field interference of the two electrode layers. To the best of our knowledge, this is the first report describing a "single" LC lens, which can modulate the focal length in both 2D and 3D modes. The proposed LC lens will be mainly used for endoscopic imaging systems.

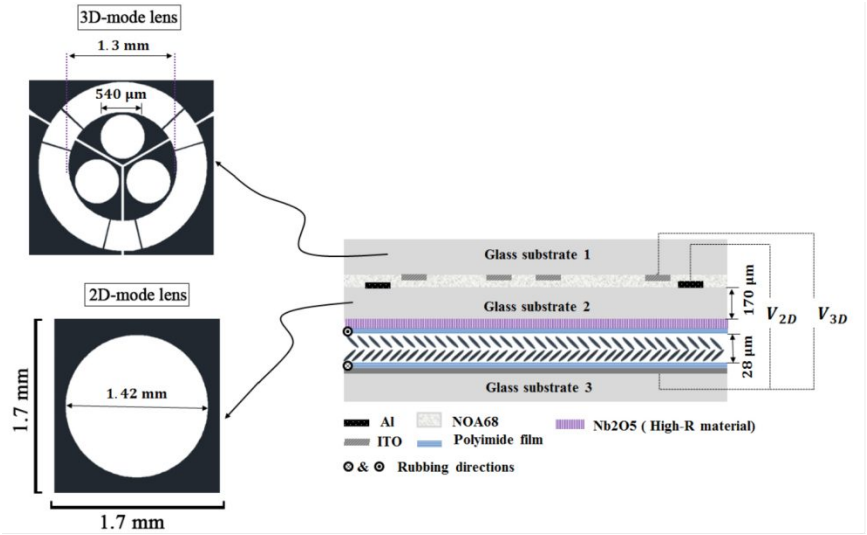

Figure 2. Top view of the electrode patterns and cross section of the MFLC-LC lens cell.

Figure 3(a) shows the interference patterns present in the 2D mode when the MFLC-lens is used with (1 kHz). In this mode only the large circular lens is activated as increasing the applied voltage, the number of the circular interference fringes changes and the property of the MFLC-lens is electrically controllable. When a 3D image is desired and multiple perspective images are needed, the electrodes in the MFLC-lens will switch to the first layer of electrode from the second layer in which there are three lenses available. As shown in Figure 3(b), the 3D lenses are obtained by applying (1 kHz). In Figure 4, the focal length of MFLC-lens as 2D mode and 3D mode are shown. It is noted that the niobium pentoxide (Nb_2O_5) has a high dielectric constant and has having high resistivity. Therefore, we expect this layer to smooth the phase profile even when the MFLC-lens is not applied with a proper frequency, which can make the high-R layer active.

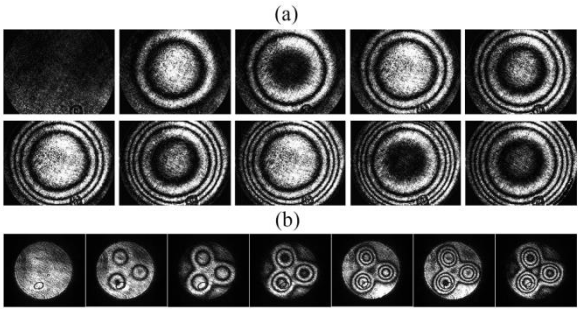

Figure 3. Interference pattern when MFLC-lens is used with different voltages (a) for 2D mode 0~12.5 Vrms (b) for 3D mode 0~8.5 Vrms.

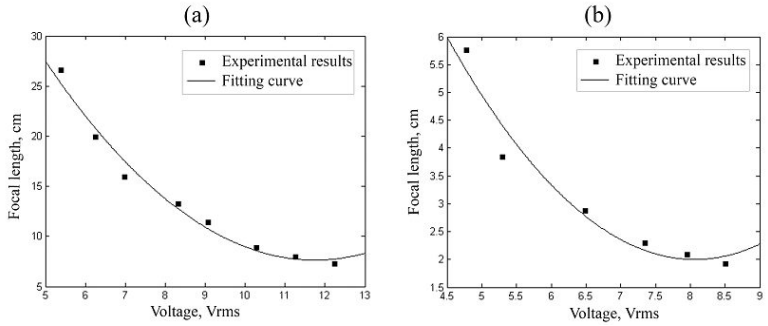

Figure 4. Focal length as a function of the applied voltage for (a) 2D mode and (b) 3D LC lens.

Figure 5 shows six images of the ISO 3334 test chart when the position of the chart is located at different distances from the MFLC-lens and when the MFLC-lens is on or off. Figure 5(a), the test chart location is 80 mm from the lens with a driving voltage of 12.5 volts. In Figure 5(b), the test chart location is 125 mm from the lens with driving voltage of 8.5 volts. In Figure 5 (c), the location is in 180 mm with driving voltage of 6.8 volts. The optical power adjustment of the MFLC-lens brings the object into focus, which leads to a sharp and clear image. Figure 5(b) illustrates the experimental setup we used to capture the images using a side viewing endoscope, for captured images shown in Figure 5(d). Each MFLC-lens can focus on the different depths of an object as the applied voltage varies without any movement for the image sensor or the CCD. The sectional 2D images can be achieved at arbitrary depth positions by altering the focal length of the MFLC-lens. The depth information data was obtained by capturing several 2D images of the 3D object. When the MFLC-lens is switched to 3D mode, each lens can capture a 2D image of the 3D object from different angles at varying tunable depths. Therefore, the system can record the depth information of the image by properly synchronizing the 2D images. A rudimentary 3D image reconstructed from a set of 2D images after object segmentation, image alignment and depth map generation is shows in Figure 5(e).

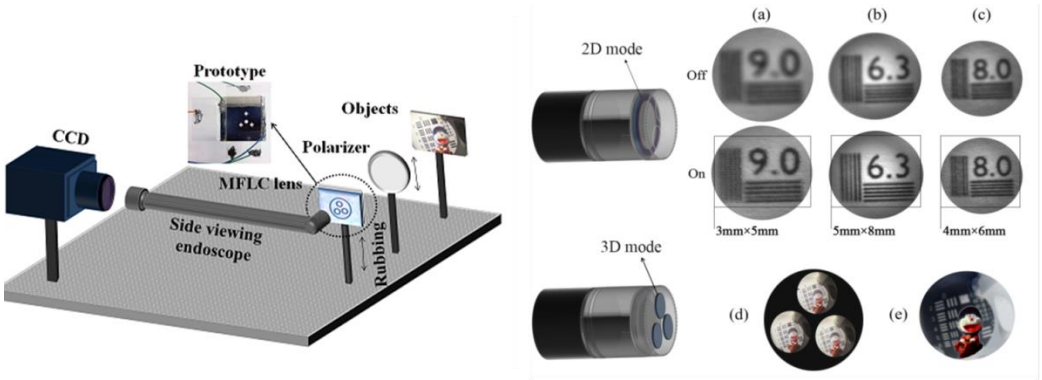

Figure 5. Image performance of the MFLC-lens for different distance of ISO 3334 test chart from the MFLC-lens when lens is on and off. Distance and voltage values are: (a) 80 mm/ 12.5Vrms (b) 125 mm/ 8.5Vrms (c) 180 mm/ 6.8Vrms. (d) three 2D images taken to construct a 3D image shown in (e).

3. 3D MICROSCOPE

In recently researches, 3D light field microscope is able to capture the light field information and reconstruct the 3D image [9-11] mechanical movement. However, depth of field (DoF) of light field microscope is usually narrow because the effective resolution decreases rapidly. To solve this problem, Perwaß and Wietzke proposed a lens array with three different focal length type lenses to extend depth of field [12]. In this paper, we proposed a tunable hexagonal liquid crystal micro-lens array (HLC-MLA) to instead of fix micro-lens array. The advantage of liquid crystal lens array is that we can adjust its focal length electrically. Therefore, the depth of field can be extended by adjusting the focal length of HLC-MLA as shown in Figure 6.

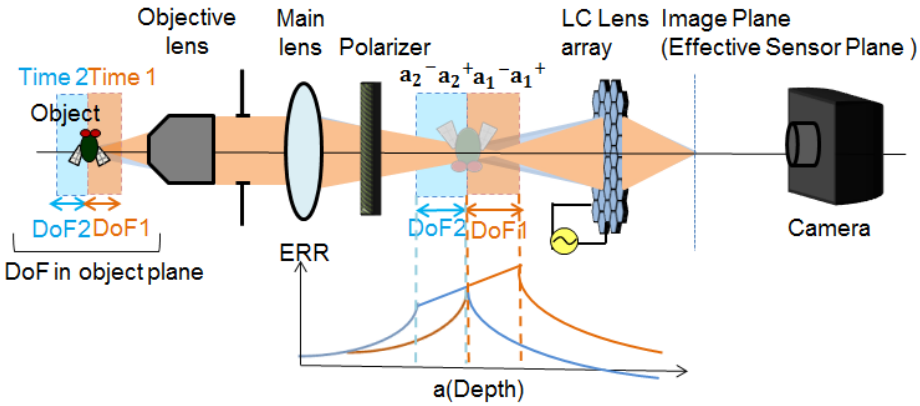

Figure 6. Principle scheme of extending DoF of 3D light field microscope implemented with HLC-MLA.

The structure of high resistance layer HLC-MLA is shown in Figure 7. The LC material was E7, LC cell gap was 60 um, and lens pitch was 350 um. There are 63×47 small hexagonal holes on the aluminum-glass substrate as micro-lens electrode pattern. The aluminum electrode width was 15 um. Then, we coat Nb_2O_5 with 20 nm thickness as high resistance layer. The hexagonal-hole aluminum electrode pattern was inside the cell to lower the driving voltage. When we applied voltage on the electrode of HLC-MLA, the refractive index variation of LC molecule would induce lens-like phase retardation in LC cell. The driving signal was a square wave. We could adjust the frequency of driving signal to control the focal length of HLC-MLA. Higher driving frequency would induce larger phase retardation difference in the LC cell, and decrease the focal length of HLC-MLA. Figure 8(a) shows the interference patterns of HLC-MLA as the focal length changing from 1.9 mm to 3.5 mm. With the high resistance layer, the fringe patterns of HLC-MLA became as concentric circles in the small hexagonal apertures. Also we could evaluate the lens quality of HLC-MLA by the profile of focal point as shown in Figure 8(b).

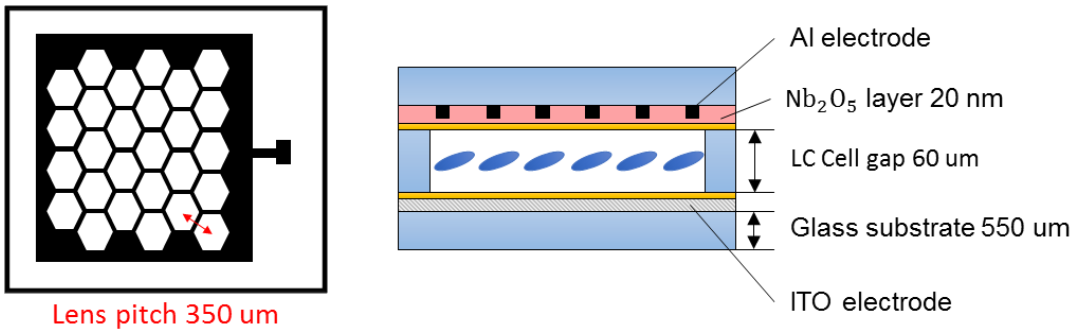

Figure 7. Top view of the electrode patterns and cross section of the HLC-MLA cell.

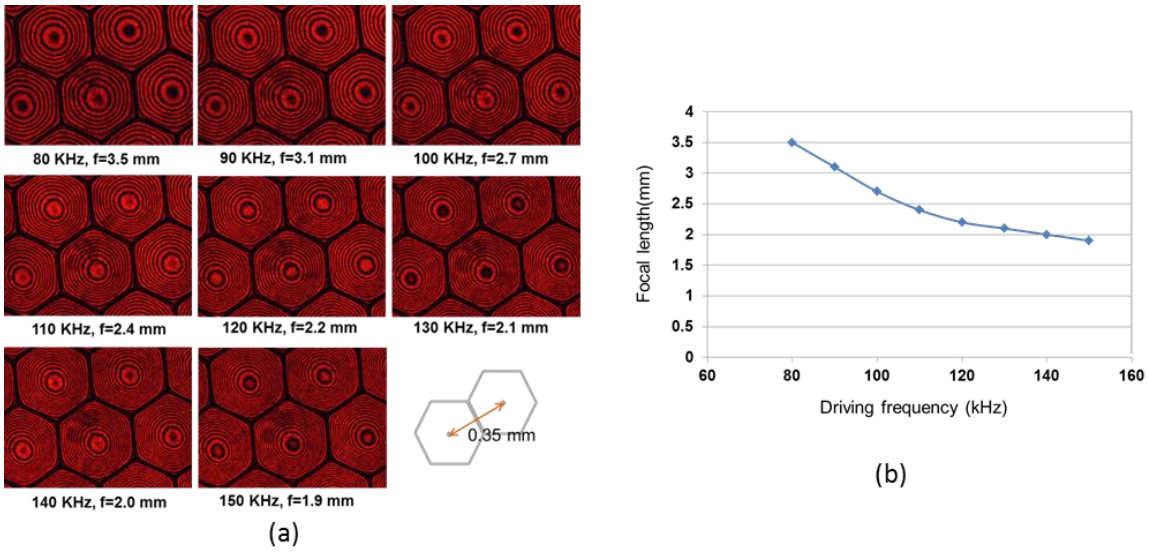

Figure 8. (a) The interference pattern of LC lens array at driving voltage 2.6 Vrms and driving freq. 80 kHz ~ 150 kHz square wave. (b) Relation between driving frequency and focal length of HLC-MLA.

In the light field microscope system, the specimen (an ant) was placed at the focal plane of objective lens, and the main lens image was at the reference plane of HLC-MLA. Figure 9(a) shows the rendering image refocusing at the front foot (depth a = 10.5 mm) with the light field image of HLC-MLA focal length f = 1.9 mm (150 kHz, 2.6 Vrms). On the other hand, as shown in Figure 9(b), the same front foot was blur on the rendering image from light field image of HLC-MLA focal length f = 3.5 mm (80 kHz, 2.6 Vrms), because its ERR was too low at that depth. Figure 9(c) shows that the light field of HLC-MLA focal length f = 1.9 mm had low ERR at the depth of back foot a = 23 mm. But, as Figure 9(d) shows, the light field image of HLC-MLA focal length f = 3.5 mm was capable to render the back foot at well image quality. By engaging rendering images from the eight light field images, DoF of light field microscope could be extended from 0.06 mm to 0.78 mm in specimen space in front of the objective lens.

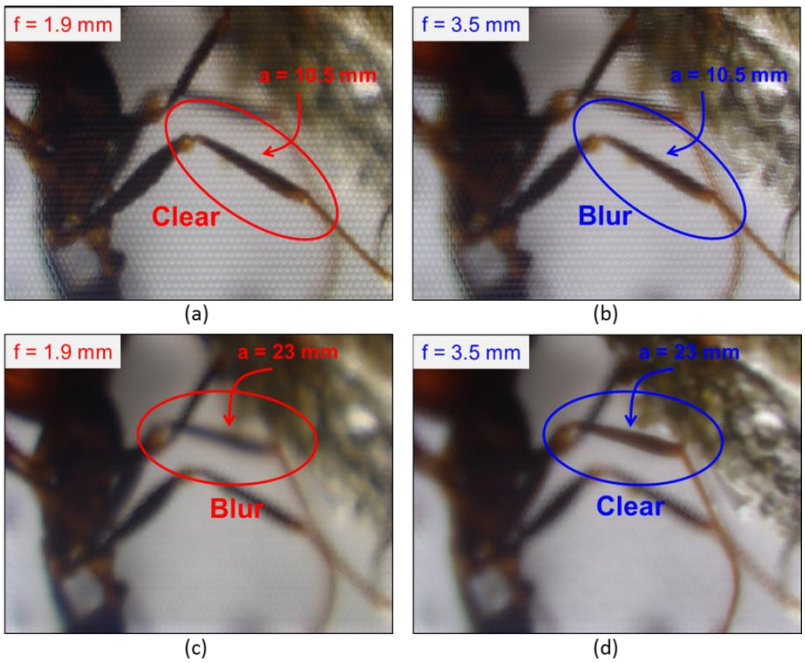

Figure 9. Rendering image with HLC-MLA focal length f = 1.9 mm refocusing at (a) a = 10.5 mm, (c) a = 23 mm; rendering image with HLC-MLA focal length f = 3.5 mm refocusing at (a) a = 10.5 mm, (c) a = 23 mm

4. CONCLUSION

In this paper, two liquid crystal (LC) lens arrays are proposed for 3D endoscope and 3D microscope system respectively. Both LC lens arrays are fabricated with a high-resistance (High-R) layer which can provide smooth electric field and well lens quality. In 3D endoscope, the multi-functional liquid-crystal lens (MFLC-lens) is demonstrated for 2D and 3D switchable function. Importantly, this MFLC-lens can further modulate the focal length without mechanical movement in both 2D and 3D modes. To achieve multiple focal length lens functions, a novel structure with dual-layer electrode was developed. The diameter of the proposed MFLC-lens is only 1.42mm with tunable focal length from infinity to 80mm. It can be easily applied to micro-imaging systems, and objects in close proximity sensing for both 2D and 3D image capturing. Applications may include medical imaging, endoscopy, robotics, and cell phones. In the 3D light field microscope, a hexagonal liquid crystal micro-lens array (HLC-MLA) with 20 nm Nb_2O_5 as high-resistance layer was coated on the Al electrode pattern. With adjusted appropriate focal length of HLC-MLA from 1.9 mm to 3.5 mm for different depth region, the effective depth of field of light field microscope was extended from 0.06 mm to 0.78 mm.

5. ACKNOWLEDGMENT

This work was financially supported by National Science Council, Taiwan, under contrasts NSC101-2221-E-009-120-MY3, and prof. Bahram Javidi under the contract no. NSF/IIS-1422179. The polyimide was kindly supported by Chisso Corporation.

6. REFERENCE

[1] S. Sato, “Liquid-crystal lens-cells with variable focal length,” Jpn. J. Appl. Phys. 18(9), 1679–1684 (1979).
[2] M. Ye and S. Sato, “Optical properties of liquid crystal lens of any size,” Jpn. J. Appl. Phys. 41(Part 2, No. 5B), L571–L573 (2002).
[3] S. Sato, “Applications of liquid crystals to variable-focusing lenses,” Opt. Rev. 6(6), 471–485 (1999).
[4] Chao-Te Lee, Yan Li, Hoang-Yan Lin, and Shin-Tson Wu, "Design of polarization-insensitive multi-electrode GRIN lens with a blue-phase liquid crystal," Opt. Express 19, 17402-17407 (2011).
[5] Hsu, CJ; Chao, PCP; Kao, YY.” A Thin Multi-Ring Negative Liquid Crystal Lens Enabled by High-k Dielectric Material,” Microsyst Technol, 17(5-7), 923-929 (2011).
[6] Chih-Wei Chen, Myungjin Cho, Yi-Pai Huang, and Bahram Javidi, “Three-dimensional imaging with axially distributed sensing using electronically controlled liquid crystal lens,” Opt. Lett. 37, 4125-4127 (2012).
[7] Yu-Cheng Chang, Tai-Hsiang Jen, Chih-Hung Ting, and Yi-Pai Huang, “High-resistance liquid-crystal lens array for rotatable 2D/3D autostereoscopic display,” Opt. Express 22, 2714-2724 (2014).
[8] M. Singer, J. Endres, A. Yetasook, W. Halabi, I. Voskresensky, M. J. Stamos, and R.Clements, “Evaluation of 3-D laparoscopy to complete surgical skills tasks,” Surgical Endoscopy: 2013 Sci. Sess.Soc. Amer. Gastrointest. Endoscop. Surgeons 27(S304–S503), 520 (2013).
[9] T. Georgiev, and C. Intwala, “Light-field camera design for integral view photography,” Tech. rep., Adobe Systems, Inc. (2006).
[10] M. Levo, R. Ng, A. Adams, M. Footer, M. Horowitz “Light Field Microscopy,” Proceedings of ACM siggraph, 25(3), 924-934 (2006).
[11] A. Lumsdaine, and T. Georgiev, “Full resolution lightfield rendering,” Tech. rep., Adobe Systems, Inc. (2008).
[12] C. Perwaß and L. Wietzke “Single lens 3D-camera with extended depth-of-field,’’ Proceedings of the SPIE 8291 (2012).